Mathematical Model Equation Development for Optimization of PVDF Membrane Surface Properties

Rasoul Moradi [a*], Hassan Niknafs [a]

[a] *Nanotechnology Laboratory, School of Engineering and Applied Sciences, Khazar University, Baku, Azerbaijan*
*Tel: +994555613482; Email: rmoradi@khazar.org

Abstract

This paper aims to develop mathematical models to optimize the surface properties of PVDF membrane modified by superhydrophobic macromolecules. The main application of these surface engineered membranes is in membrane distillation for treatment of water and desalination purposes. Response surface methodology (RSM) was applied in the variables and their independent and concert responses on the surface features. To achieve this goal, the three-level three-factorial Box–Behnken experimental design was chosen for finding out the relationship between the response functions (contact angle, pore size and overall porosity) and variables (PVDF concentration, SMM concentration and solvent evaporation time).

1.   Introduction

Membrane distillation (MD) is a non-isothermal membrane operation in which the driving force is the partial vapor pressure difference across the porous and hydrophobic membrane. MD has potential application for desalination purposes and is successfully employed in other fields such as waste-treatment and food industry [1,2]. One of the main advantages of MD is to operate in the moderate temperatures and pressures. There is a temperature difference between two sides of the membrane make the permeate flux through the hydrophobic membrane. Regarding to the low operation temperatures in such a process, various cheap energy sources, like solar energy and waste heat, could be used. This is a key point in the application of expensive separation processes such as desalination [3-5]. In this process, diffused vapour molecules are transformed into cold product using four different methods: (a) a cold liquid in direct contact with the membrane

(DCMD), (b) a cold surface separated from the membrane by an air gap (AGMD),
(c) a cold sweeping gas (SGMD), or (d) a vacuum (VMD) (Fig. 1) [6].
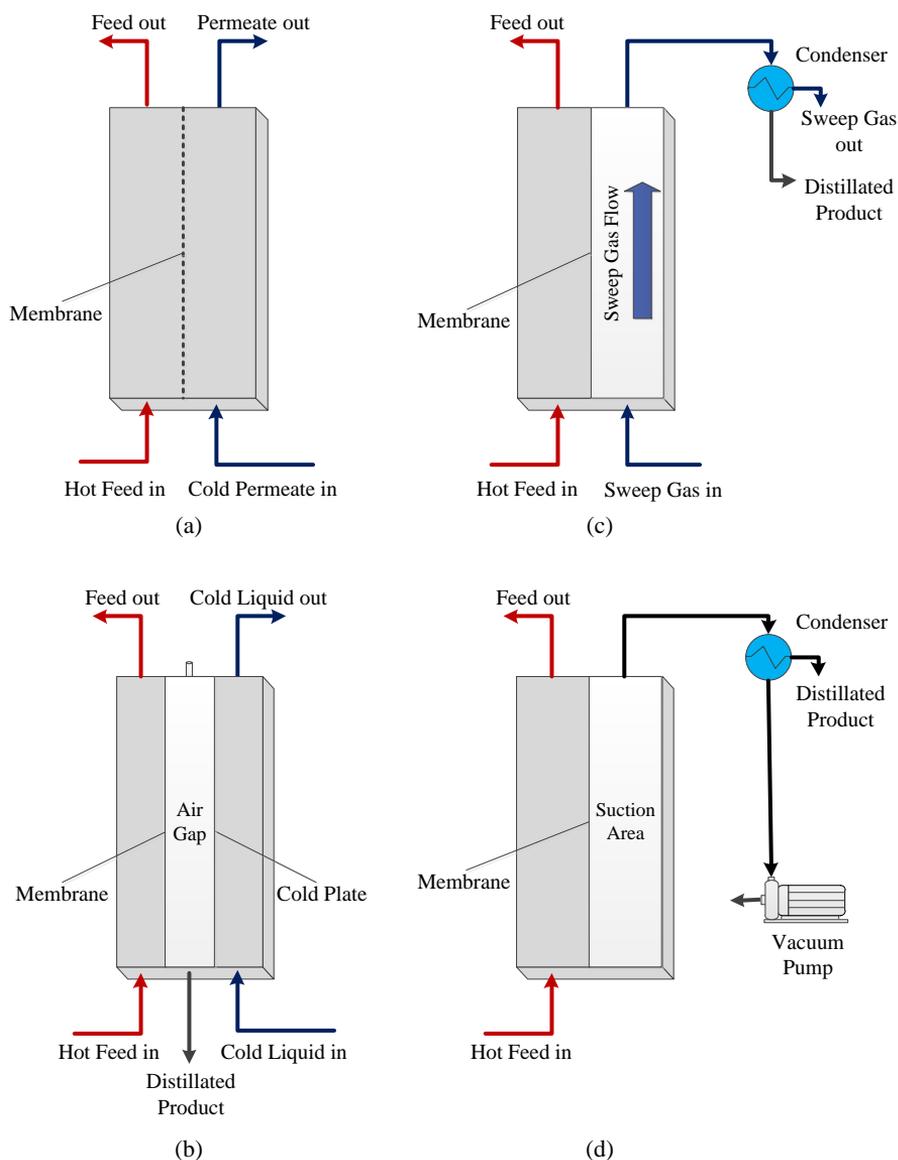
Fig. 1. Membrane distillation configuration: (a) DCMD; (b) AGMD; (c) SGMD; (d) VMD.

2.   Materials and Methods

Table 1 summarizes the materials used together with molecular structure and their
chemical abstract service (CAS) number.

Table 1 Materials used for preparation of modified PVDF membranes.

Material Description	CAS Number	Molecular structure/Liner Formula	Source
4,4´-Methylene bis(phenyl isocyanate) (MDI, 98%)	101-68-8	$CH_2(C_6H_4NCO)_2$	Sigma–Aldrich, Inc., St. Louis, MO, USA
1H,1H,2H,2H-Perfluoro-1-decanol (PFD, Mw = 464.12, 97%)	678-39-7	$CF_3(CF_2)_7CH_2CH_2OH$	Sigma–Aldrich, Inc., St. Louis, MO, USA
Poly(vinylidene fluoride) Average M_w ~530,000, pellets	24937-79-9	$(CH_2CF_2)_n$	Sigma–Aldrich, Inc., St. Louis, MO, USA
Sodium chloride (NaCl)	7647-14-5	NaCl	Sigma–Aldrich, Inc., St. Louis, MO, USA
Tetrahydrofuran (THF, HPLC grade 99.9%)	109-99-9	C_4H_8O	Sigma–Aldrich, Inc., St. Louis, MO, USA
Poly (propylene glycol) (PPG, M_n= 425)	25322-69-4	$H[OCH(CH_3)CH_2]_nOH$	Sigma–Aldrich, Inc., St. Louis, MO, USA
N,N-Dimethylacetamide (DMAc, anhydrous 99.8%)	127-19-5	$CH_3CON(CH_3)_2$	Merk
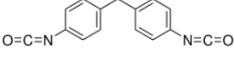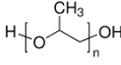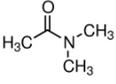
3. Results and Discussion

3.1 SMM and membrane synthesis and characterization

SMM was synthesized using conventional polyurethane chemistry. Methylene bis(p-phenyl isocyanate) (MDI) use as the backbone of polymeric chain and was

reacted with poly(propylene glycol) (PPG) as a polyalcohol. The produced oligomeres end caped appropriate fluoroalcohol of 1H,1H,2H,2H-Perfluoro-1-decanol (PFD), Prepared samples were dried in an oven at 50°C for 5 days. The molar mixing ratio of the chemicals MDI:PPG:PFD was 3:2:2.

For the synthesized SMM, the number (M_n) and weight (M_w) average molecular weights, and the index of the molecular weight distribution (M_w/M_n) were measured by gel permeation chromatography (GPC) (GPC Agilent 1100-RID, USA) at 30 ºC. SMM was dissolved in THF and filtered with a 0.45 μm filter to remove high molecular weight components. Polystyrene was used as the calibration standard.

The obtained functional groups of the obtained pre-polymer and SMM were investigated by a Fourier transform infrared spectrometer (FTIR, Brucker 3020, Germany) in the range 4000–400 cm^{-1}. At the end of each step, 1ml of each solution was placed under vacuum to remove the solvent until they became viscose. Finally, two drops of each solution was dropped onto the KBr discs.

In order to measure the contact angle of SMM polymer, a solution with 12 wt. % of SMM in DMAC was prepared and cast on a glass plate to a thickness of 0.3 mm. The cast film together with the glass plate was placed in a vacuum drying oven maintained at 60 ºC until the solvent was completely evaporated. For lowering the effects of pores and surface roughness the dense film of SMM was prepared and the water contact angle was measured by a contact angle goniometer (JYSP360, united test, China).

Flat-sheet membranes were prepared by the phase-inversion method. First, PVDF was dissolved in DMAC (12.0 wt. %) and stirred at 50 ˚C for about 12 h to ensure the complete dissolution of the polymer. Then the prepared solution was used to prepare the pristine PVDF membranes. For the preparation of PVDF/SMM membranes, different concentrations of SMM were dissolved into the prepared PVDF casting solutions and the solutions were allowed to stir at ambient temperature for at least 8 h. The mixture was then degassed over night at room temperature. The polymer solutions were cast on a smooth glass plate to a thickness of 0.25 mm using a motorized film applicator with a casting speed of 1 m/min. The solvent was then evaporated at room temperature for a predetermined period (0, 3 and 6 min) before the cast films were immersed together with the glass plates for 1 day in distilled water at 22˚C.

During coagulation, the membrane spontaneously peeled off the glass substrate. The membranes were firstly immersed in an aqueous ethanol solution 33 wt. % for 1h, then in an aqueous ethanol solution 66 wt. % and finally in pure ethanol for 2h.

Furthermore, the membranes were dried at room temperature for 1 day to complete the drying process.

The cross-section and top surface of the membranes were analyzed by the scanning electron microscope (SEM, Hitachi Model S 4100, Japan) equipped with the energy dispersive X-ray spectrometer (EDX, Oxford Instruments, USA). First, the membrane sample was fractured in liquid nitrogen and then sputter-coated with a thin layer of gold.

In order to find out the effect of SMM on the membrane properties, the cross-section was analyzed by X-ray energy dispersion spectroscopy (EDX) to determine the nitrogen, fluorine, carbon and oxygen content throughout the membrane cross-section using the software INCA (Oxford Instruments, USA). The distribution of nitrogen elements over membrane cross-section can be viewed using element maps. Element mapping utilizes the X-ray signal from a specified energy range in order to show the elemental distribution. The mean pore size of the top membrane surfaces (SEM pictures) were measured by Image Tool picture analysis software (UTHSCSA).

Contact angles of deionized water on the top and bottom surfaces of the membranes were measured by a contact angle goniometry (JYSP360, united test, China) at room temperature. In this study, the reported contact angle was the average of three different measurements.

In order to find the overall porosities, the membranes were placed in isopropanol for 1 day until it is fully penetrated, then the membrane porosities were measured by determining their swelling in isopropanol using the following expression

$$\varepsilon = \frac{W2 - W1}{S.\,d.\,\rho} \tag{1}$$

Where ε is membrane overall porosity, W_1 and W_2 are weights of the membranes in the dry and wet states, respectively; S and d represent the area and the average thickness of the membrane in the wet state, respectively and ρ is stand for the density of isopropanol at room temperature.

3.2. MD Experiments

DCMD and AGMD experimental set-up used to test the permeation performance of the prepared optimum membrane for desalination. Both the feed and permeate circulated through the membrane module by means of a double-head peristaltic pump (Watson Marlow, 323). The temperature of the feed solution was controlled

by a heating thermostat (501A, Shanghai experimental instrument Co., LTD,
China) and that of the distillate water was controlled by a cooling thermostat
(DTY-10A, Beijing Detianyou technology development Co., LTD, China). The
inlet temperature of the feed solution into the module was maintained at three
different temperature (68, 75 and 83°C) for two different feed concentration (0.5
and 1 mol/lit) for both DCMD and AGMD. The effective membrane area of both
DCMD and AGMD systems was 0.49×10^{-3} m^2. Figure 10 of the main text shows
the set-up used to conduct the DCMD experiments. In the DCMD configuration,
hot feed solution was brought into contact with the top layer of the membrane and
the cold permeate solution is in contact with the bottom layer of the membrane.
The temperature of the cold distillate water in DCMD was kept at 15 °C. Figure 2S
shows schematic of AGMD experimental set-up. In the AGMD configuration,
evaporated water molecules at the liquid /membrane interface cross the membrane
pores and the air gap chamber to finally condense over the cooling stainless steel
metallic plate. The temperature of the cold plat in AGMD was kept at 15 °C.
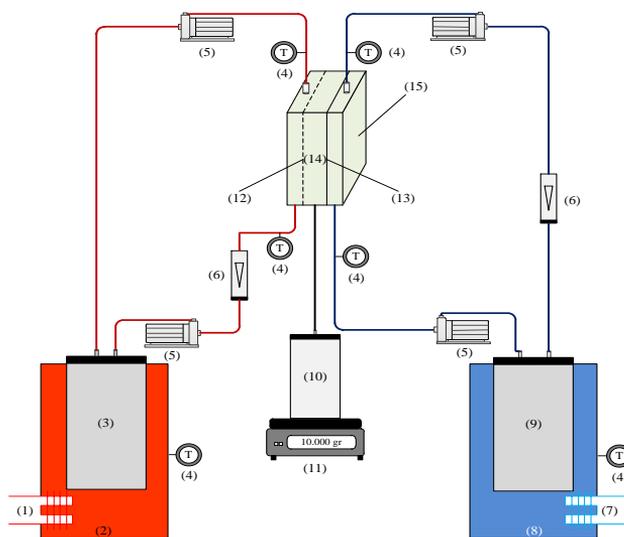
Fig. 2. Schematic of AGMD experimental set-up (1) Water heater (2) Hot water bath (3)
Feed tank (4) Thermocouple (5) Peristaltic pump (6) Flow meter (7) Water Cooler (8) Cold
water bath (9) Cooling liquid (10) Permeate tank (11) Balance (12) Membrane (13) Cold
plate (14) Air gap (15) AGMD module

It should be mentioned that each of the DCMD and AGMD experimental tests
were carried out for 2 hr. At the end, the MD conditions for reaching higher flux
were found. Finally, the optimum modified membrane and the unmodified
membrane at same preparation condition but without SMM additive were used in
MD experiment under the higher MD flux conditions to see the effect of SMM

addition on permeate flux and salt rejection. Permeation flux of the membranes was calculated by the following equation:

$$J = \frac{W}{A.t} \qquad (2)$$

Where J is the pure water flux ($Kg/(m^2 \cdot h)$), W is the permeation mass of water (Kg), A is the effective membrane areas (m^2), t is the sampling time (h). The solute rejection (R) of membrane was obtained from the following equation:

$$R = \left(1 - \frac{C1}{C2}\right) \times 100\% \qquad (3)$$

Where c_1 and c_2 are the solute concentration of permeate and feed solution, respectively that measured by water quality meter (Model 900, BANTE Co., China).

3.3. Range of PVDF concentration

When the polymer content of the precursor solution is less than a threshold value (e.g. 10 wt. % for PVDF), large holes appear within the membrane that strongly will effect on the membrane performance (selectivity).

(a)   (b)
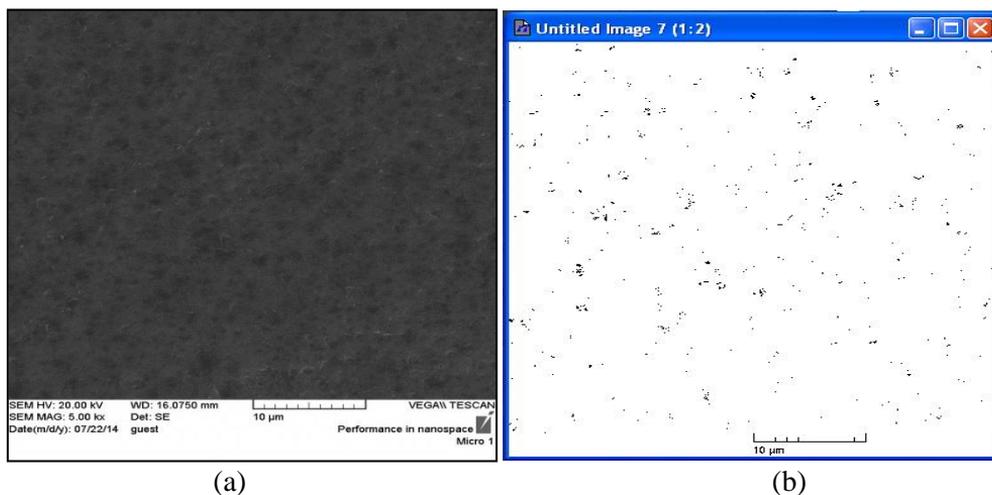
Fig. 3. The influence of PVDF high concentration on decreasing of the porosity and pore size of the membrane surface, (a) SEM image and (b) image analyses of pore distribution on the surface of PVDF/SMM (20/1 wt.%) , without considering the evaporation time.

On the other hand, by increasing the base polymer concentration in the PVDF/SMM solution, viscosity of the polymer solution will be increased which slowed down SMM migration to the top membrane surface. It was observed that the membrane prepared by 12 wt. % PVDF (without SMM and considering the evaporation time effects), is fragile with poor surface features. Where in the case of 20 wt. % PVDF, at the same synthesize condition, the obtained membrane surface was smooth with low porosity. By addition 1.0 wt. % SMM into this membrane due to weak SMM migration toward the surface, the thick skin layer with small pores (~90 nm) formed. The SEM and image analyzing results illustrated in Fig.3S confirm this observation.

3.4. Range of SMM concentration

| (a) | (b) |
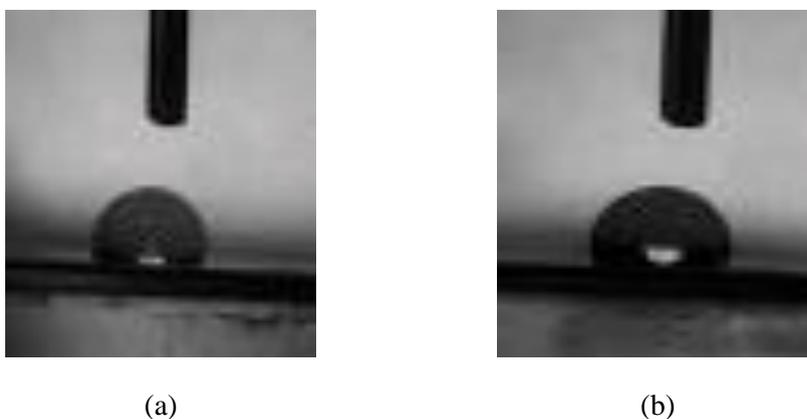
Fig. 4. Water contact angle images of 12 wt. % PVDF membranes(a) 4 wt. %.of SMM, CA=110˚, (b) 2 wt. %.of SMM, CA=112˚,

In the preparation of modified membranes to avoid altering the bulk properties and also to create a very thin hydrophobic layer on top of the membrane, less than 4 wt. % SMM usually was used. In addition, it was reported that the polymeric surfaces would take only a certain amount of SMM. In fact the saturation of surface take place in high SMM concentration. As a result increasing of the SMM concentration up to these certain levels does not increase the percentage composition of the membrane surface anymore. On the other words, the surface properties get independent from SMM IN high concentration .In relevant works it was seen that at SMM concentrations of about 2 wt. %, the PVDF membrane surface is saturated. It was reported that the appropriate value of SMM concentration is around 0.5 wt. %.

In this work we employed two range of SMM concentrations as 2 and 4 wt. %,(in the 12 wt. % PVDF and evaporation time of 1 min). Then the effects of SMM

concentration changes on the membrane surface hydrophobicity were studied through water contact angle measurements. Results show that by 2 fold increasing in the SMM concentration (from 2 wt. %. to 4 wt. %.), the significant changes in water CA of the membrane surface have not been seen. The correspondent CA images are represented at Fig.4.

3.5. Range of Evaporation time

As mentioned, SMM migration occurs only in polymer solution and migration stops after the phase separation process. As a result, prior to the coagulation, certain period of time is required for SMM migration to the surface of the membrane. Increasing in the casting bath temperature and evaporation time both strongly affect the SMM migration from the membrane bulk to surface. However, CA analyses indicate that after a period of elapsed time during the evaporation the SMM concentration in the membrane surface does not change (Fig. 5). In this manner, the water contact angle of the membrane surface gets fixed because of the saturation of the surface with SMM. In addition, the increasing in the evaporation time results in the thickening of the membrane skin layer. This results in the low porosity of the membrane. Moreover, the formation of skin layer diminish the surface roughness and pore size as well as hydrophobicity.

(a)   (b)
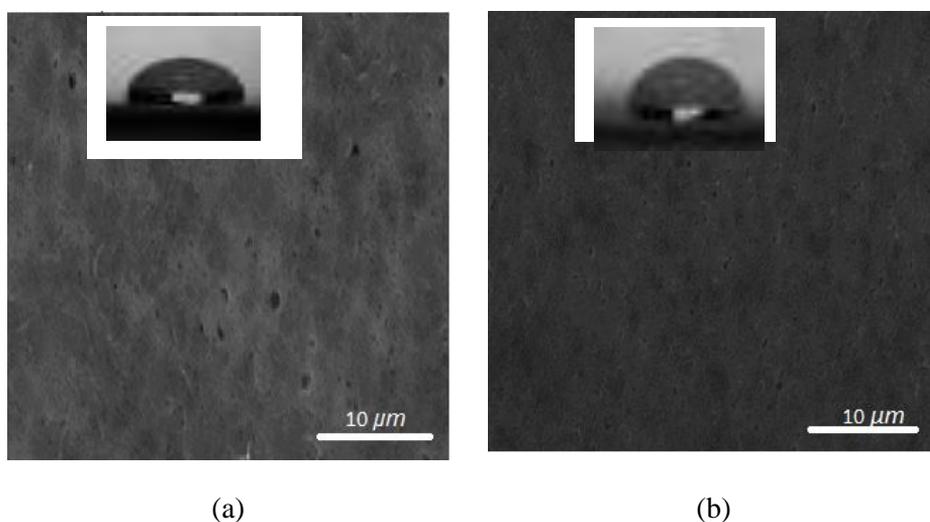
Fig. 5. Surface contact angle and morphology of as prepared membranes, (a) for 6 min of evaporation time: ε=73% and CA= 108˚, (b) for 8 min of evaporation time ε=69% and CA=106˚. (ε and CA stand for porosity and water contact angle respectively).

Here for evaluating the influence of evaporation times on the surface
hydrophobicity and porosity, two types of membranes were prepared in the various
times of evaporation (6 and 8 min). The water CA and porosity measurements were
conducted for both types of membranes. It was observed that by increasing of the
evaporation time from 6 min up to 8 min there is no delectable variations in the
water CA values. However, the porosity of the membrane surface strongly
decreased due to increasing in the thickness of formed skin layer.

3.6. Box–Behnken design

Response surface methodology (RSM) was applied in the variables and their
independent and concert responses on the surface features. To achieve this goal, the
three-level three-factorial Box–Behnken experimental design was chosen for
finding out the relationship between the response functions (contact angle, pore
size and overall porosity) and variables (PVDF concentration, SMM concentration
and solvent evaporation time) [8,9].

Independent variables and their levels for the Box–Behnken design used in this
study are shown in Table 2.

Table 2 The level of variables chosen for the Box-Behnken design

Variable	Symbol	Coded variable level		
		Low	Center	High
		-1	0	1
PVDF concentration (wt. %)	X_1	12	15	18
SMM concentration (wt. %)	X_2	0	1	2
Evaporation time (min)	X_3	0	3	6

The second-order polynomial equation could be used to define the behavior of the
system as following:

$$Y = \beta_0 + \sum_{i=1}^{k} \beta_i x_i + \sum_{i=1}^{k} \beta_{ii} x_i^2 + \sum_{i=1}^{k-1} \sum_{j=2}^{k} \beta_{ij} x_i x_j + \varepsilon \tag{4}$$

Wherein Y stands for predicted responses (Y_1 = surface contact angle, Y_2 = mean
surface pore size, Y_3 = overall porosity).In the case of present problem of three
independent variables, the Eq. (4) is simplified as following:

$$Y = \beta_0 + \beta_1 x_1 + \beta_2 x_2 + \beta_3 x_3 + \beta_{11} x_1^2 + \beta_{22} x_2^2 + \beta_{33} x_3^2 + \beta_{12} x_1 x_2 + \beta_{13} x_1 x_3 + \beta_{23} x_2 x_3 + \varepsilon \tag{5}$$

Where x_1, x_2 and x_3 stand for input variables; β_0 is a constant; β_1, β_2 and β_3 are linear coefficients; β_{11}, β_{22}, β_{33} are quadratic coefficients; β_{12}, β_{13}, β_{23} are interactions and ε is noise or error.

In the present work, a Box-Behnken statistical design with three factors and three levels was employed to fit second order polynomial model which indicated that 13 experiments were required for this procedure (Table 3). The Design-Expert software (version 9, Stat-Ease Inc., Minneapolis, USA) was used for model regression, plotted figures, and optimization. The P values of less than 0.05 were considered to be statistically significant [10,11].

3.7. Mathematical Model and Optimization of Modified PVDF membranes

Response surface optimization is more advantageous than the traditional single parameter optimization as it saves time, space and raw material. Thirteen experiments were performed to investigate the effects of the PVDF concentration (x_1), SMM concentration (x_2), solvent evaporation time (x_3) and their interactions on the responses (Y_1: contact angle, Y_2: mean pore size, Y_3: porosity).Independent variables and their levels for the Box–Behnken design used in this study are shown in Table 2.

Using the relationships in Table 2, the actual levels of the variables for each of the experiments in the design matrix were calculated and experimental results obtained as given in Table 3.

Table 3. Box–Behnken design with actual/coded values for three size fractions and results

Run no.	Actual and coded level of variables			Experimental responses		
	X_1(wt. %)	X_2(wt. %)	X_3(min)	Y_1 (°)	Y_2 (µm)	Y_3 (%)
1	18 (+1)	1 (0)	6 (+1)	112.52	0.11	67.85
2	12 (-1)	2 (+1)	3 (0)	112.86	0.14	78.50
3	15 (0)	2 (+1)	6 (+1)	115.00	0.12	67.70
4	18 (+1)	0 (-1)	3 (0)	86.50	0.15	74.50
5	18 (+1)	2 (+1)	3 (0)	110.61	0.11	70.60
6	12 (-1)	0 (-1)	3 (0)	86.20	0.23	82.04
7	15 (0)	2 (+1)	0 (-1)	107.80	0.13	80.42
8	18 (+1)	1 (0)	0 (-1)	102.30	0.12	74.64
9	15 (0)	1 (0)	3 (0)	105.25	0.15	76.40
10	12 (-1)	1 (0)	6 (+1)	114.77	0.14	75.28
11	12 (-1)	1 (0)	0 (-1)	103.41	0.19	83.43
12	15 (0)	0 (-1)	6 (+1)	86.25	0.18	72.50
13	15 (0)	0 (-1)	0 (-1)	86.00	0.19	79.64

The analysis of variance (ANOVA) for three responses was given in Table 4S. The
P value higher than 0.95 was considered as the threshold of parameter elimination
in the response model equation calculations. The significance of each coefficient
was determined by P value. The P value less than 0.05 indicates that model terms
are significant. It was determined that the quadratic model was acceptable for
responses and R^2 and R_{adj}^2 indicate good agreement with the experimental data. As
mentioned before, all the following figures were plotted using Design-Expert
software, and in all presented figures, the other factor was kept at level zero
(medium level).

Table 4. Analysis of variance (ANOVA) quadratic model

Source	Contact Angle (°) Regression coefficients	P-value	Pore Size (µm) Regression coefficients	P-value	Overall Porosity (%) Regression coefficients	P-value
Intercept	*105.25*		*0.15*		*76.15*	
X_1	*-0.66*	*0.4961*	*-0.026*	*0.0006*	*-3.96*	*0.0005*
X_2	*12.66*	*0.0001*	*-0.031*	*0.0003*	*-1.43*	*0.0201*
X_3	*3.63*	*0.0150*	*-0.010*	*0.0196*	*-4.35*	*0.0003*
$X_1 X_2$	*-0.64*	*0.6383*	*0.013*	*0.0290*	*-0.090*	*0.8760*
$X_1 X_3$	*-0.28*	*0.8316*	*1.000E-002*	*0.0560*	*0.34*	*0.5640*
$X_2 X_3$	*1.74*	*0.2385*	*2.944E-019*	*1.0000*	*-1.39*	*0.0615*
X_1^2	*1.64*	*0.3074*	*-3.750E-003*	*0.4216*	*0.25*	*0.7035*
X_2^2	*-7.85*	*0.0050*	*0.011*	*0.0550*	*0.012*	*0.9845*
X_3^2	*1.36*	*0.3874*	*-6.250E-003*	*0.2103*	*-1.10*	*0.1440*

Table 5. Model equations for contact angle, pore size, overall porosity.

Responses	Model Equation	Eq.	F-value	P-value	R^2	R_{adj}^2
Contact angle	$Y_1 = 105.25 - 0.66X_1+12.66X_2+3.63X_3-0.64 X_1 X_2-0.28 X_1 X_3+1.74 X_2 X_3+1.64 X_1^2-7.85 X_2^2+1.36 X_3^2$	(6)	29.22	0.0027	0.9850	0.9513
Pore size	$Y_2 = 0.15-0.026X_1-0.031X_2-0.010X_3+0.013X_1X_2+1.000E-002X_1X_3+2.944E-3.750E-003X_1^2+0.011X_2^2-6.250E-003X_3^2$	(7)	31.34	0.0023	0.9860	0.9546
Porosity	$Y_3 = 76.15-3.96X_1-1.43X_2-4.35X_3-0.090X_1X_2+0.34X_1X_3-1.39X_2X_3+0.25X_1^2-1.10X_3^2$	(8)	29.01	0.0027	0.9849	0.9510

From experimental results, the second-order response functions representing
responses can be expressed as a function of the PVDF concentration (x_1), SMM
concentration (x_2) and the solvent evaporation time (x_3). Table 5 presents the
relationship between responses (y_1, y_2 and y_3) and variables were obtained for

coded unit for three size fractions. The responses at any regime in the interval of our experiment design could be calculated from Eqs. (4) – (5).

Conclusion

The three-level three-factorial Box–Behnken experimental design was chosen for finding out the relationship between the response functions (contact angle, pore size and overall porosity) and variables (PVDF concentration, SMM concentration and solvent evaporation time). For the first time we successfully developed the mathematical model equations for optimization of contact angle, porosity and pore size of surface modified membranes.

References

[1] D.E. Suk, G. Chowdhury, T. Matsuura, R.M. Narbaitz, P. Santerre, G. Pleizier, Y. Deslandes, Study on the kinetics of surface migration of surface modifying macromolecules in membrane preparation, Macromolecules. 35 (2002) 3017–3021.

[2] Y.W. Tang, J.P. Santerre, R.S. Labow, D.G. Taylor, Use of surface-modifying macromolecules to enhance the biostability of segmented polyurethanes, J. Biomed. Mater. Res. 35 (1997) 371–381.

[3] Y.W. Tang, J.P. Santerre, R.S. Labow, D.G. Taylor, Synthesis of surface-modifying macromolecules for use in segmented polyurethanes, J. Appl. Polym. Sci. 62 (1996) 1133–1145.

[4] M. Tomaszewska, Preparation and properties of flat-sheet membranes from polyvinylidene fluoride for membrane distillation, Desalination 104 (1996) 1–11.

[5] R.S. Ward, K.A., White, C.B. Hu, Use of surface-modifying additives in the development of a new biomedical polyurethaneurea. In: H. Planck, G. Egbers, I. Syré (Eds.), Polyurethanes in Biomedical Engineering, Elsevier, Amsterdam, 1984.

[6] M. Shin, Y.H. Lee, M.M. Rahman, H. Kim, Synthesis and properties of waterborne fluorinated polyurethane-acrylate using a solvent /emulsifier-free method, Polymer. 54 (2013) 4873-4882

[7] R. Moradi, J. Karimi, M. Shariati-Niassar, M. A. Koochaki, Preparation and characterization of Polyvinylidene fluoride/graphene superhydrophobic fibrous films, Polymers 7 (2015) 1444-1463.

[8] Y.W. Tang, J.P. Santerre, R.S. Labow, D.G. Taylor, Application of macromolecular additives to reduce the hydrolytic degradation of polyurethanes by lysosomal rnzymes, Biomaterials, 18 (1997) 37.

[9] Z. Ge, X. Zhang, J. Dai, W. Li, Y. Luo, Synthesis, characterization and properties of a novel fluorinated polyurethane. Eur. Polym. J. 45 (2009) 530–536.

[10] G. Manvia, Arvind R. Singhb, Ramanand N. Jagtapa, D.C. Kotharib, Isocyanurate based fluorinated polyurethane dispersion for anti-graffiti coatings, Prog. in Org. Coat.75 (2012) 139–146.

[11] T. Liu, L. Ye, Synthesis and properties of fluorinated thermoplastic polyurethane elastomer. J. of Fluor. Chem. 131 (2010) 36–41.